ISBN: 978-3-95450-231-8 ISSN: 2673-5490 doi: 10.18429/JACoW-IPAC2023-WEPL112

SIMULTANEOUS COMPENSATION OF THIRD-ORDER RESONANCES AT THE FNAL RECYCLER RING

C. E. Gonzalez-Ortiz*, P. N. Ostroumov[1], Michigan State University, East Lansing, USA
R. Ainsworth, Fermilab, Batavia, USA
[1] also at FRIB, East Lansing, USA

Abstract

Third-order resonance lines will have a detrimental effect on the high-intensity operation of the Recycler Ring (RR), under the current Proton Improvement Plan (PIP-II) for the Fermilab Accelerator Complex. Increasing intensity will increase space charge effects, leading to the excitation of normal and skew sextupole lines. Dedicated normal and skew sextupoles have been installed in order to mitigate the effect of these resonance lines. By measuring the response matrix of the third-order Resonance Driving Terms (RDTs) to the currents of these dedicated elements, this study shows how several resonance lines can be compensated simultaneously. Resonance compensation is experimentally verified through loss maps and emittance growth measurements using the Ion Profile Monitor (IPM) system in the Recycler.

INTRODUCTION

As the Fermilab Accelerator Complex enters the Proton Improvement Plan II (PIP-II) era, new challenges arise for high-intensity operation. The objective of delivering a 1.2 MW proton beam to the Deep Underground Neutrino Experiment (DUNE) through the Long-Baseline Neutrino Facility (LBNF) will require several upgrades to the accelerator complex. This include the addition of an 800-MeV superconducting linear accelerator, as well as several upgrades to the downstream accelerators, including the Booster Ring, Recycler Ring and Main Injector [1, 2]. The layout of the current and future accelerator complex is shown in Fig. 1.

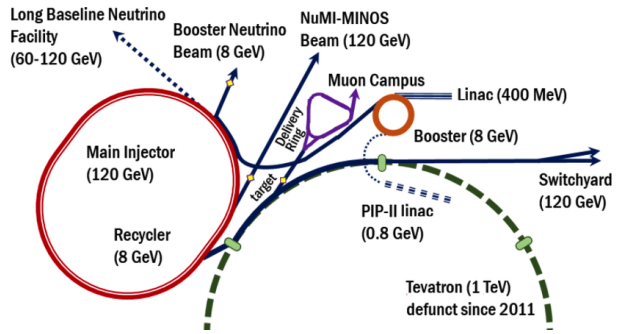

Figure 1: The past (Tevatron), present and future (PIP-II and LBNF) of the FNAL Accelerator Complex, taken from [3].

As intensity is increased, the space charge tune shift will lead to the excitation of third-order resonance lines around the operation point of the Recycler Ring [1,4]. The nominal operation point for the tune is $Q_x = 25.43$ for the horizontal plane and $Q_y = 24.42$ for the vertical. Correspondingly, the resonance lines of interest are $3Q_x = 76$ and $Q_x + 2Q_y = 74$, which come from normal sextupole excitation. In addition, there are skew sextupole lines with equations $3Q_y = 73$ and $2Q_x + Q_y = 75$. Figure 2 shows a loss map for the tune region close to operation. The brighter regions in the plot correspond to regions where more losses occur. The first thing to note is that the coupling line $Q_x - Q_y = 1$ is already being corrected for with skew quadrupoles. Furthermore, the third-order lines can be superimposed onto the loss map, coinciding with the regions of beam loss. This work explores the simultaneous compensation of these resonance lines.

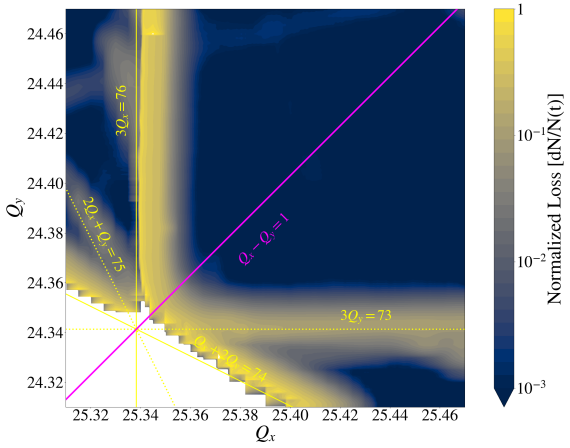

Figure 2: Loss map for the Recycler Ring with third-order resonance lines superimposed.

COMPENSATION OF RESONANCES

Resonance Driving Terms

Previous studies in the Recycler Ring have shown the measurements of the Resonance Driving Terms (RDTs) [5], in accordance to the general theory of RDTs as described in Ref. [6]. Table 1 shows how each RDT can be associated to each resonance line. Table 1 also specifies the first-order source for each resonance, and, ultimately, the correction element needed, i.e., either a normal or skew sextupole.

The RDT will quantify the strength of the resonance lines. Therefore, by cancelling out the real part and the imaginary part of each RDT, one can effectively compensate each resonance. This will significantly reduce beam losses at these resonance regions. Figure 3, shows how by introducing appropriate kicks one can bring the global h_{3000} term to 0.

In general, RDTs are defined by the order in which they enter the one-turn normal form Hamiltonian [6]. The general

* gonza839@msu.edu

This manuscript has been authored by Fermi Research Alliance, LLC under Contract No. DE-AC02-07CH11359 with the U.S. Department of Energy, Office of Science, Office of High Energy Physics.

ISBN: 978-3-95450-231-8 ISSN: 2673-5490 doi: 10.18429/JACoW-IPAC2023-WEPL112

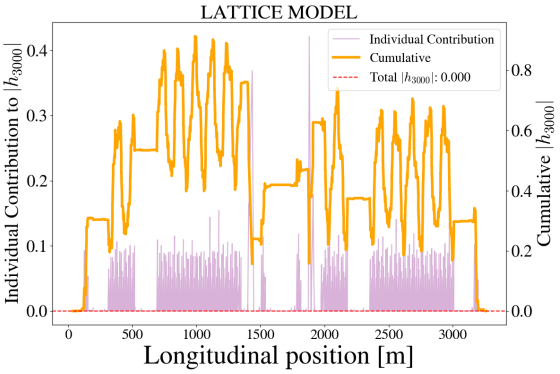

Figure 3: Individual correction for the h_{3000} term and local contributions calculated from the lattice model.

Table 1: Corresponding RDTs and Source for Each Third-order Resonance Line

Resonance Line	RDT	Source
$3Q_x = 76$	h_{3000}	Normal Sextupole
$Q_x + 2Q_y = 74$	h_{1020}	Normal Sextupole
$3Q_y = 73$	h_{0030}	Skew Sextupole
$2Q_x + Q_y = 75$	h_{2010}	Skew Sextupole

expression to define RDTs reads:

$$h_{jklm} = \Xi_{jklm} \sum_i L_i \beta_{xi}^{\frac{j+k}{2}} \beta_{yi}^{\frac{l+m}{2}} V_{ni} e^{i\left[(j-k)\phi_{xi}+(l-m)\phi_{yi}\right]}, \tag{1}$$

where Ξ_{jklm} is just a constant defined as:

$$\Xi_{jklm} = -\frac{q}{p_0}\frac{1}{2^n}\frac{1}{n}\binom{n}{l+m}\binom{j+k}{j}\binom{l+m}{l}. \tag{2}$$

For Eqs. (1) and (2), $n = j + k + l + m$ represents the order of the resonance. The sum over i is done over all multipoles of order n and length L_i that either have a normal component $V_{ni} = B_{ni}$ if $l + m$ is even, or a skew component $V_{ni} = A_{ni}$ if $l + m$ is odd. The symbols for β_{xi}, β_{yi}, ϕ_{xi} and ϕ_{yi} represent the beta funtions and phase advances in each plane, respectively. Figure 3 plots compensated h_{3000}, which reads:

$$h_{3000} = -\frac{q}{p_0}\frac{1}{24}\sum_i L_i \beta_{xi}^{\frac{3}{2}} B_{3i} e^{3i\phi_{xi}}. \tag{3}$$

Compensation of Third-Order Resonances

For resonance compensation we have four dedicated normal sextupoles with currents that can be set to $(I_{sc220}, I_{sc222}, I_{sc319}, I_{sc321})$ and four dedicated skew sextupoles with currents that can be set to $(I_{ss323}, I_{ss323}, I_{ss319}, I_{ss321})$. As shown in the previous section one RDT can be cancelled out with the right kick from the correction elements, which means the resonances are corrected to first order.

Nevertheless, by compensating one resonance line, other resonances might become worse. This is why for simultaneous compensation, compensation currents will vary depending on the subsets of resonances to compensate. In principle, the currents I_x needed in each correction element in order to cancel out the four bare machine RDTs, are given by the solution to this linear system of equations:

$$\begin{pmatrix} -|h_{3000}|\cos\psi_{3000} \\ -|h_{3000}|\sin\psi_{3000} \\ -|h_{1020}|\cos\psi_{1020} \\ -|h_{1020}|\sin\psi_{1020} \\ -|h_{0030}|\cos\psi_{0030} \\ -|h_{0030}|\sin\psi_{0030} \\ -|h_{2010}|\cos\psi_{2010} \\ -|h_{2010}|\sin\psi_{2010} \end{pmatrix}_{(Bare)} = \boldsymbol{M} \begin{pmatrix} I_{sc220} \\ I_{sc222} \\ I_{sc319} \\ I_{sc321} \\ I_{ss223} \\ I_{ss323} \\ I_{ss319} \\ I_{ss321} \end{pmatrix}, \tag{4}$$

where M_{ij} is the response matrix for the RDTs with respect to the currents, and includes any roll that can happen for the correction sextupoles. This response matrix M_{ij} can be calculated by scanning the currents in each correction element and looking at the response from the real and imaginary part of the RDTs, i.e., $h_{jklm} = |h_{jklm}|e^{i\psi_{jklm}}$. Alternatively, the response matrix can also be calculated theoretically from the lattice model, by means of Eq. (1). For the Recycler Ring, both methods predict similar currents for individual compensation of RDTs.

In reality, there are limitations to solving Eq. (4). The first one is that all the RDTs (h_{jklm}) may not be accessible for measurement, given that they may not show up as a spectral line. See Ref. [5] for the method used to measure RDTs at the Recycler Ring. Another limitation is that the solution for the currents may be outside of the maximum limits for the correction elements.

One can also try to cancel out a subset of RDTs from Eq. (4). For example, in order to compensate $3Q_x = 76$ and $Q_x + 2Q_y = 74$ simultaneously with the normal sextupoles, the system of equations to be solved is:

$$\begin{pmatrix} -|h_{3000}|\cos\psi_{3000} \\ -|h_{3000}|\sin\psi_{3000} \\ -|h_{1020}|\cos\psi_{1020} \\ -|h_{1020}|\sin\psi_{1020} \end{pmatrix}_{(Bare)} = \boldsymbol{M} \begin{pmatrix} I_{sc220} \\ I_{sc222} \\ I_{sc319} \\ I_{sc321} \end{pmatrix}. \tag{5}$$

Figures 4 and 5 allow for visualization of the solutions to Eq. (5). If the currents from the solution are introduced into the correction elements in the lattice, one can verify that the h_{3000} and the h_{1020} are globally adjusted to zero. There are regions where the local contributions to the h_{3000} are relatively high to bare machine values. Experimentally, the currents needed for this compensation exceed the maximum limits that can be set to correction elements. Nevertheless, other subsets of resonances can be compensated simultaneously, as can be seen in Fig. 6.

EXPERIMENTAL VERIFICATION

Loss Maps

As mentioned before, loss maps are a powerful tool to characterize resonances and their compensation. In particular, Fig. 6 shows how by solving a subset of equations from

ISBN: 978-3-95450-231-8 ISSN: 2673-5490 doi: 10.18429/JACoW-IPAC2023-WEPL112

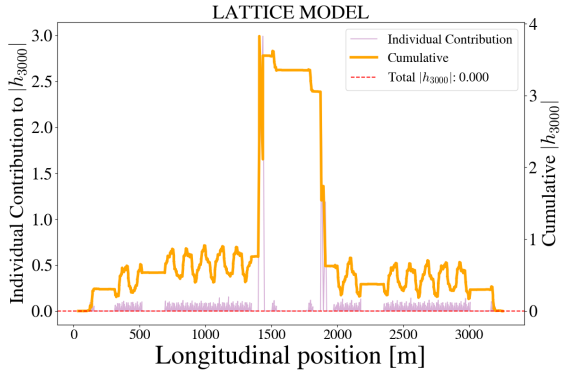

Figure 4: Profile for h_{3000} term around the ring with $3Q_x = 76$ and $Q_x + 2Q_y = 74$ compensation.

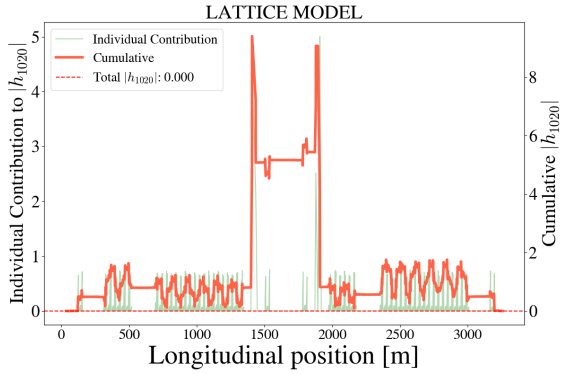

Figure 5: Profile for h_{1020} term around the ring with $3Q_x = 76$ and $Q_x + 2Q_y = 74$ compensation.

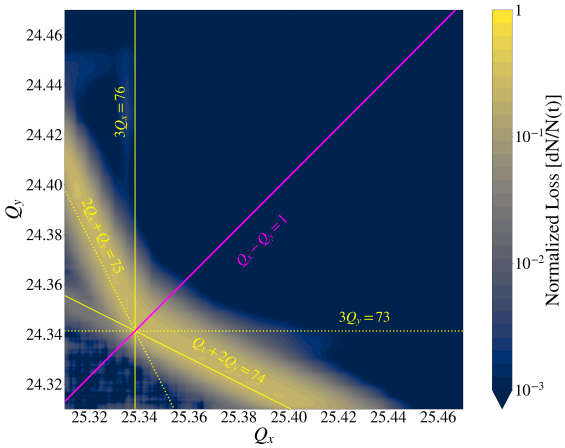

Figure 6: Tune map scan with optimal compensation currents in corrector elements for $3Q_x$ and $3Q_y$ compensation.

Eq. (4), the beam losses around the resonances are decreased. Figure 6 can be compared to the bare machine loss map in Fig. 2. It can be seen that the losses around the $3Q_x = 76$ and $3Q_y = 73$ regions have decreased significantly.

Static Tune Scan

Another tool to visualize resonance compensation are static tune scans. For the loss maps described in the previous section the crossing of the resonance happens dynamically. Another approach is to set the tune at a certain value and measure the beam survival ratio, as well as the beam size for a certain window of time. The beam size is measured using the Ion Profile Monitor System (IPM) in the ring and is reported in arbitrary units, just to show a relative effect.

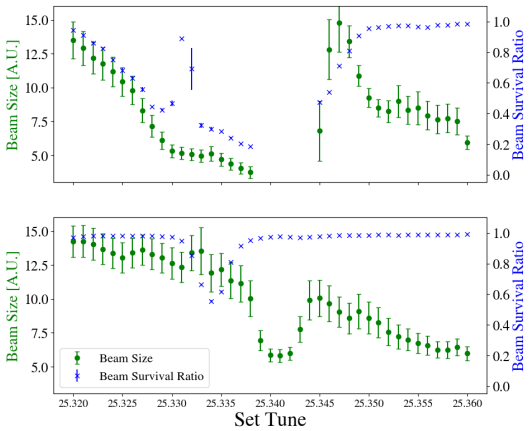

Figure 7: Measurements of beam size and beam survival ratio by means of static tune scans for bare machine (top) and with $3Q_x = 76$ compensation (bottom).

The top plot in Fig. 7 shows a static tune scan with no resonance compensation. No beam survives on top of the resonance and the beam size also starts blowing up as we approach the resonance. Nevertheless, when the currents that cancel out h_{3000} are set (bottom plot), the beam survival ratio around $3Q_x = 76$ increases. There is a valley for the beam size at this region, but this may be an artifice from the Gaussian fit. If beam tails are amplified by the compensation, the Gaussian fit will not give the best fit. Further investigation into this effect is underway.

CONCLUSIONS

The RDT method can be extended to compensate multiple resonance lines. Nevertheless, there will be a limit set by the maximum currents in the correction elements. There will also be a limit for when the sextupole component is no longer a perturbation, and the assumption for the RDT expansion breaks down.

ACKNOWLEDGEMENTS

This manuscript has been authored by Fermi Research Alliance, LLC under Contract No. DE-AC02-07CH11359 with the U.S. Department of Energy, Office of Science, Office of High Energy Physics. We would like to acknowledge the ASET (Accelerator Science and Engineering Traineeship) program at Michigan State University. The ASET program is partially supported by the US Department of Energy, Office of Science, High Energy Physics under Cooperative Agreement award number DE-SC0018362 and Michigan State University.

ISBN: 978-3-95450-231-8 ISSN: 2673-5490 doi: 10.18429/JACoW-IPAC2023-WEPL112

REFERENCES

[1] R. Ainsworth *et al.*, "High intensity space charge effects on slip stacked beam in the Fermilab Recycler", *Phys. Rev. Accel. Beams*, vol.22, p. 020404, 2019. doi:10.1103/PhysRevAccelBeams.22.020404

[2] R. Ainsworth *et al.*, "High intensity operation using proton stacking in the Fermilab Recycler to deliver 700 kW of 120 GeV proton beam", *Phys. Rev. Accel. Beams*, vol.23, p. 121002, 2020. doi:10.1103/PhysRevAccelBeams.23.121002

[3] J. Eldred, V. Lebedev and A. Valishev, "Rapid-cycling synchrotron for multi-megawatt proton facility at Fermilab", *J. Instrum.*, vol. 14, p.07021, 2019. doi:10.1088/1748-0221/14/07/P07021

[4] R. Ainsworth *et al.*, "Improvements to the Recycler/Main Injector to Deliver 850 kW+", in *Proc. NAPAC'22*, Albuquerque, New Mexico, United States, Oct. 2022. doi:10.18429/JACoW-NAPAC2022-WEYE3

[5] C. E. Gonzalez-Ortiz *et al.*, "Third Order Resonance Compensation at the FNAL Recycler Ring", in *Proc. IPAC'22*, Bangkok, Thailand, Jun. 2022, pp. 195–198. doi:10.18429/JACoW-IPAC2022-MOPOST050

[6] R. Bartolini and F. Schmidt, "Normal form via tracking or beam data", *Part. Accel.*, vol. 59, pp. 93–106, 1998. https://cds.cern.ch/record/333077